The Effect of Sliding Humeral Osteotomy (SHO) on Frontal Plane Thoracic Limb Alignment: An Ex Vivo Canine Cadaveric Study

Adam H. Breiteneicher[1], Bo Norby[2], Kurt S. Schulz[3], Sharon C. Kerwin[1], Don A. Hulse[1], Derek B. Fox[4], and W. Brian Saunders[1]

[1]Department of Small Animal Clinical Sciences, Texas A&M University, College Station, Texas, [2]Department of Large Animal Clinical Sciences, Michigan State University, East Lansing, Michigan, [3]Peak Veterinary Referral Center, Williston, Vermont, and [4]Department of Veterinary Medicine and Surgery, University of Missouri, Columbia, Missouri

Corresponding Author
W. Brian Saunders
Texas A&M University
4474 TAMU
College Station, TX 77843-4474
bsaunders@cvm.tamu.edu

Submitted June 2016
Accepted July 2016

DOI:10.1111/vsu.12574

Objective: To determine the effect of sliding humeral osteotomy (SHO) on frontal plane thoracic limb alignment in standing and recumbent limb positions.
Study Design: Canine cadaveric study.
Sample Population: Canine thoracic limbs (n=15 limb pairs).
Methods: Limbs acquired from healthy Labrador Retrievers euthanatized for reasons unrelated to this study were mounted in a limb press and aligned in a standing position followed by axial loading at 30% body weight. Frontal plane radiography was performed in standing and recumbent positions pre- and post-SHO. In the standing position, lateralization of the foot was measured pre- and post-SHO using a textured grid secured to the limb press base plate. Twelve thoracic limb alignment values (mean ± SD and 95% CI) were determined using the center of rotation of angulation (CORA) method were compared using linear mixed models to determine if significant differences existed between limb alignment values pre- or post-SHO, controlling for dog, limb, and limb position.
Results: Six of 12 standing or recumbent alignment values were significantly different pre- and post-SHO. SHO resulted in decreased mechanical lateral distal humeral angle and movement of the mechanical humeral radio-ulnar angle, radio-ulnar metacarpal angle, thoracic humeral angle, and elbow mechanical axis deviation toward coaxial limb alignment. In the standing position, the foot underwent significant lateralization post-SHO.
Conclusion: SHO resulted in significant alteration in frontal plane thoracic limb alignment. Additional studies are necessary to determine if the changes reported using our ex vivo model occur following SHO in vivo.

The presence of medial coronoid disease of the canine elbow with concurrent widespread medial joint compartment osteoarthritis (OA) is often referred to as medial compartment disease (MCD).[1–7] The severe cartilage erosions that occur with MCD in the presence of apparently healthy joint surfaces of the lateral joint compartment have led some authors to draw similarities between canine MCD and medial knee gonarthrosis in people.[8,9] One treatment for medial knee gonarthrosis is a high tibial osteotomy, designed to transfer loads from the diseased medial knee compartment to the less severely affected lateral joint compartment.[10–12]

The sliding humeral osteotomy (SHO) was developed to treat MCD of the canine elbow by transferring loads from the severely affected medial compartment toward the lateral joint compartment.[8,13] In the ex vivo setting, SHO has been reported to alter joint surface contact areas and to reduce the force applied to the proximal articular surface of the ulna 25–28% by transferring force to the articular surface of the radius.[8,13] When assessed using subjective and objective outcome measures, SHO improved or resolved lameness in dogs with MCD as early as 12–26 weeks after surgery.[14] More recently, force plate analysis was used to document a significant improvement in lameness in 60 elbows (46 dogs) by 12 weeks after SHO.[15] SHO case selection guidelines remain somewhat subjective, particularly for veterinarians not familiar with the procedure.[4]

In people, the center of rotation of angulation (CORA) method is used to diagnose, classify, and plan surgical corrections of proximal tibial varus associated with medial knee gonarthrosis.[10–12,16,17] Importantly, it is necessary for limb alignment values to be determined with the limb in a loaded, or weight bearing, position. For this reason, radiographs are obtained on people in a standing position.[17–20] Although the CORA method has been successfully adapted to canine

Presented at the Veterinary Orthopedic Society Annual Conference, Big Sky, MT, March 2016.

orthopedics, many of these studies have been performed with limbs in recumbent positions.[21–23] To mimic the standing radiographic position used in people, we previously developed a technique to obtain thoracic limb frontal plane radiographs in standing and recumbent dogs.[24] The CORA method was used to report reference ranges for 12 thoracic limb alignment values in healthy Labrador Retrievers and document significant differences in limb alignment values in standing and recumbent limb positions.[24]

Based on prior studies in people[10–12,16,17] and ex vivo contact mechanics studies in the canine elbow,[8,13] we propose that SHO alters joint contact mechanics not only by direct translation of joint surfaces adjacent to the osteotomy, but also through alteration of frontal plane thoracic limb alignment. Therefore, the objective of this study was to determine if there were significant differences in thoracic limb alignment values in response to SHO using ex vivo simulated standing and recumbent limb positions. We adopted the null-hypothesis that there would be no significant differences in limb alignment values pre- vs. post-SHO when determined from radiographs obtained in either standing or recumbent positions.

MATERIALS AND METHODS

Specimen Acquisition and Preparation

Fifteen pairs of thoracic limbs (30 limbs total) were acquired from healthy, skeletally mature Labrador Retrievers (23–50 kg body weight) euthanatized for reasons unrelated to this study. As this study involved cadaveric limbs, Institutional Animal Care and Use Committee approval was not required at the site of study. Each limb was dissected free from the thorax and stored in specimen bags at −20°C. Limb pairs were thawed at room temperature for 12–16 hours prior to testing. Craniocaudal, 90° flexed, and standard mediolateral radiographic projections were obtained of each elbow joint to screen for any evidence of elbow dysplasia, OA, pre-existing trauma, or other musculoskeletal abnormalities. Additionally, exploratory arthrotomy was performed on each specimen after completion of the testing protocol to determine if gross evidence of joint pathology was present. Identification of any abnormality on pre-study radiographs or post-study exploratory arthrotomy resulted in exclusion of the limb and its pair.

For each limb, skin and subcutaneous tissues were dissected from the proximal scapula to the carpus. The triceps muscle and tendon of insertion were removed. The subscapularis, supraspinatus, infraspinatus, teres major and minor, biceps brachii, brachialis, shoulder joint capsule, and elbow joint capsule remained undisturbed. A 3.5 mm diameter eye screw was placed in the caudal scapular neck in a caudocranial direction at the level of the origin of the long head of the triceps muscle. Another eye screw was placed similarly in the olecranon at the insertion of the triceps. An in-series turnbuckle and extension spring (Part 1NAN8, K-Coefficient 21.17 kN/m, W.W. Grainger, Inc, Lake Forest, IL) were secured between to the 2 screws to simulate the triceps myotendinous unit. A 3.5 mm external fixator pin (Imex, Longview, TX) was placed in the cranial scapular neck in a craniocaudal direction. A second pin was placed in the greater tubercle of the humerus in a similar manner. Pin placement was performed so that both pins were parallel and in the sagittal plane. An extension spring (Part 91669747, K-Coefficient 11.09 kN/m, MSC Industrial Supply, Melville, NY) was then secured to the 2 pins to simulate the shoulder extensors and counter-balance the load applied by the triceps spring and turnbuckle apparatus.

In preparation for limb press loading, a length of the polyvinyl chloride (PVC) pipe was cut to match the length of the scapula. In order to ensure that the working length of the scapula was maintained, the scapula was transected such that 50% of the length remained and the length of the PVC pipe ended at the proximal aspect of the original scapula, maintaining the total length of the scapula. The PVC pipe was secured to the medial aspect of the remaining scapular segment using two 3.5 mm locking screws.

Limb Press and Pre-SHO Radiography

Each limb was secured in a custom-designed limb press (Southwest Research Institute, San Antonio, TX) by securing the PVC pipe previously fixed to the scapular spine to an upper test fixture attached to a loading platform (Fig 1). The loading platform was positioned such that the shoulder, elbow, and carpus could be positioned in normal flexion or extension under a standing load.[8,25–27] Importantly, the manus was allowed to freely contact the textured base plate of the limb press in an unrestrained manner. Axial alignment of the humeral head and manus was confirmed by use of a plumb line deployed from the loading platform. This plumb line was used to center the manus in a craniocaudal direction beneath the humeral head as occurs in standing dogs. Iron weights were added to the upper deck of the test fixture platform until 30% body weight was achieved. Sagittal plane joint angles were re-evaluated and the triceps turnbuckle readjusted until standing joint angles were achieved. Next, longitudinal and transverse index marks were created on the PVC pipe adjacent to the upper test fixture as reference points to ensure identical limb position in relation to the limb press after SHO (Fig 1). Lastly, to evaluate the position of the manus relative to the base plate pre- and post-SHO, the starting position of the manus was determined by marking the position of the manus on a 1 cm × 1 cm textured grid adhered to the weight bearing surface of the limb press. Three points were measured on each foot pre- and post-SHO: (1) a point equidistant between the cranial aspects of the 3rd and 4th digital pads; (2) the lateral contact point of the 5th digital pad; and (3) the caudal most contact point of the metacarpal pad. The lateral displacement of these 3 points were measured pre- and post-SHO and a mean of this displacement was calculated. This mean value was the pre-SHO foot lateralization measurement for each specimen. This process was repeated post-SHO.

A 25 mm spherical calibration tool (Akucal, J2 Medical, Pittsburgh, PA) was attached to the radiographic table and

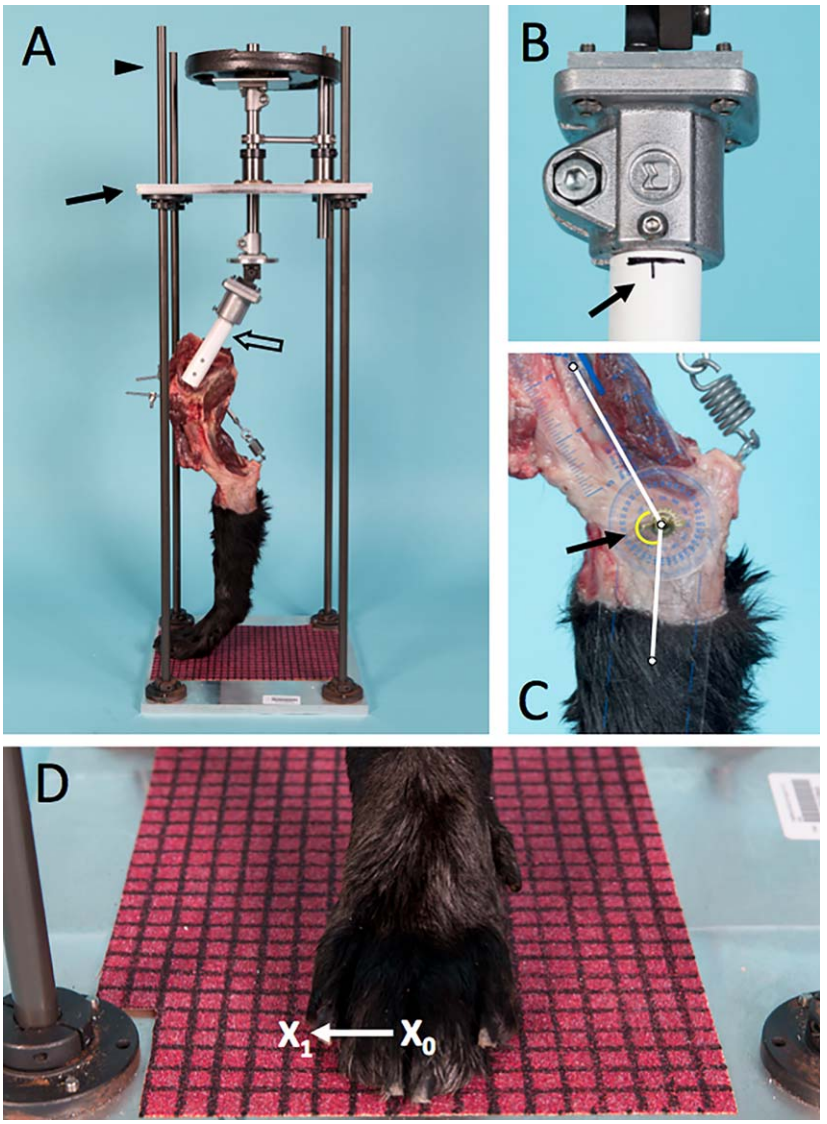

Figure 1 A custom limb press was designed and fabricated to mount and position limbs in simulated standing position. (A) Mediolateral perspective of the limb press illustrating specimen position. Arrow denotes the adjustable loading deck. Arrowhead denotes the load platform and associated iron weight. Open arrow denotes the PVC tubing secured within the upper test fixture. (B) Craniocaudal view of the upper test fixture and associated PVC tubing. The arrow denotes vertical and longitudinal index marks on PVC pipe created to ensure that position of the scapula and proximal humerus were identical upon re-mounting each specimen after sliding humeral osteotomy (SHO). (C) A goniometer was placed over the center of each joint and used to confirm normal standing joint position after loading. Arrow denotes 145° of elbow extension. (D) Photograph illustrating the 1 cm × 1 cm textured grid beneath a loaded limb. This grid was used to determine the position of the manus pre- and post-SHO. X_0 denotes pre-SHO position, whereas X_1 denotes post-SHO position.

positioned adjacent to the lateral epicondyle of the elbow. Two caudocranial radiographs (1 proximal and 1 distal) were obtained of each limb as previously described.[24] First, a proximal segment radiograph was obtained with the beam centered on the distal diaphysis of the humerus, including the shoulder and elbow joints. Next, a distal segment radiograph was obtained with the beam centered on the proximal diaphysis of the radius and ulna, including the elbow and digits. Radiographs were evaluated for correct positioning using normal anatomic landmarks and by confirming that the elbow rotation position (ERP) was 40–45%.[21]

To obtain recumbent images, each limb was removed from the limb press and placed in mediolateral recumbency on an elevated foam support. The proximal and distal aspects of the limb were manually tensioned to maximally extend the joints of the thoracic limb, simulating the technique used for recumbent horizontal beam radiography in a previous in vivo study.[24] After positioning the calibration tool, 2 caudocranial radiographs (proximal and distal) were obtained as described above. All radiographs were performed by a single resident investigator (AHB).

SHO and Post-SHO Radiography

All limbs received an SHO stabilized with a 10 mm SHO plate (New Generation Devices, Glen Rock, NJ) based on the described SHO surgical technique.[14,15] A medial approach to the humerus was performed. The SHO procedure was completed according to the current published surgical technique.[15] Caudocranial and lateral humerus radiographs were obtained to confirm proper execution of the SHO and to evaluate for complications such as improper osteotomy position, incomplete translation of the distal humerus, or plate- and screw-associated complications. Abnormalities, if present, resulted in removal of the limb and its associated pair from the study.

To simulate the stance phase after SHO, each limb was re-mounted in the upper test fixture of the limb press. To ensure the scapula and proximal humerus were positioned in an identical manner to pre-SHO standing position, the previously generated transverse and longitudinal index marks were aligned with the collar of the test fixture (Fig 1). The manus was once again allowed to freely contact the textured base plate of the limb press in an unrestrained manner and the previously described plumb line was used to confirm craniocaudal alignment. The limb was loaded as described above and the angles of the shoulder, elbow, and carpus reconfirmed.

The decision to allow the manus to lateralize in an unrestrained manner in the post-SHO standing position was made after thoughtful consideration and a pre-study pilot series involving 5 limbs evaluated in 2 post-SHO simulated standing (loaded) positions: (1) manus centered beneath the humeral head to ensure complete axial alignment of the limb and axial loading post-SHO, and (2) manus allowed to lateralize in response to SHO to mimic the clinical observations of SHO surgeons. Radiographs were performed post-SHO using these 2 positions in order to determine if lateralization of the manus, when considered alone as a component of our post-SHO loading protocol, would have a significant effect on limb alignment values in the simulated standing position. For the pilot study, limb montages were generated and limb alignment values were determined as described in detail below. Results were compared using paired t-tests with significance established at $P \leq .004$ (see statistical methods below).

Based on the results of the pilot study, post-SHO standing radiographs were completed in an identical manner to pre-SHO images. Lateral deviation of the manus relative to the sagittal plane was once again determined to evaluate the effect of SHO on lateralization of the foot. The limb was removed from the limb press and post-SHO recumbent radiographs were obtained in an identical manner to pre-SHO radiographs.

Generation of Thoracic Limb Montages and Determination of Limb Alignment Values

The proximal and distal radiographs from standing, pre-SHO limb positions were digitally merged as previously described using computer-imaging software (Adobe Photoshop CS6, Adobe Systems, Inc, San Jose, CA) to create a full-length thoracic limb digital montage.[24] Briefly, image magnification was normalized by adjusting image size until the 2.5 cm spherical calibration tool was of identical size on proximal and distal radiographic projections. Once magnification was normalized, the distal limb radiographic projection was digitally maneuvered so that the humerus, elbow, and proximal radius and ulna exactly matched the same structures on the proximal radiographic projection. Individual limb montages were saved. This process was repeated for recumbent pre-SHO images, standing post-SHO images, and recumbent post-SHO images, resulting in 120 caudocranial radiographic montages for the 15 limb pairs (30 total limbs) used in the full study. Montages were randomized and blinded for limb and limb position. A digital block was placed over the humeral diaphysis in each montage to blind for the presence or absence of the humeral osteotomy and SHO implants. All images were analyzed by 1 resident investigator (AHB) (eFilm version 3.3, Sound™, Carlsbad, CA) to determine 12 frontal plane limb alignment values for each radiographic montage using the CORA method as previously reported.[24]

Mechanical axes and joint reference lines were determined from the caudocranial radiographic montages. Mechanical axis of the humerus: A circle was centered on the humeral head such that it was congruent with the scapulohumeral joint and medial and lateral cortices of the humeral head. The joint orientation line of the distal humerus was defined as a line extending from the distolateral aspect of the humeral capitulum to the distomedial aspect of the humeral trochlea. The mechanical axis of the humerus was defined by a line connecting the center of the proximal circle to the midpoint of the joint orientation line of the distal humerus. Mechanical axis of the radius/ulna: The joint orientation line of the proximal radius/ulna was defined as a line extending from the proximomedial aspect of the ulna to the proximolateral aspect of the radial head. The joint orientation line of the distal radius/ulna was defined as a line extending from lateral articular surface of the radius to the radial styloid process. The mechanical axis of the radius/ulna was defined by a line connecting the midpoints of these 2 joint orientation lines. Mechanical axis of the carpus/metacarpus: The mechanical axis of the carpus/metacarpus was defined by a line connecting the midpoint of the distal radius/ulna joint orientation line to the midpoint between the center of the distal epiphyses of the 3rd and 4th metacarpal bones. Thoracic limb mechanical axis: The thoracic limb mechanical axis was defined by a line connecting the center of the circle positioned over the proximal humerus proximally to the midpoint between the center of the distal epiphyses of the 3rd and 4th metacarpal bones distally.

Using the mechanical axes and joint orientation lines described above, 12 mechanical (m) joint and limb alignment values were measured. (1) Mechanical lateral distal humeral angle (mLDHA): The angle lateral to the mechanical axis of the humerus defined by the intersection of the mechanical axis of the humerus and the joint orientation line of the distal humerus. (2) Mechanical medial proximal

radioulnar angle (mMPRUA): The angle medial to the mechanical axis of the radius/ulna defined by the intersection of the mechanical axis of the radius/ulna and the joint orientation line of the proximal radius/ulna. (3) Mechanical lateral distal radioulnar angle (mLDRUA): The angle lateral to the mechanical axis of the radius/ulna defined by the intersection of the mechanical axis of the radius/ulna and the joint orientation line of the distal radius/ulna. (4) Mechanical lateral proximal carpal metacarpal angle (mLPCMCA): The angle lateral to the mechanical axis of the carpus and metacarpus defined by the intersection of the mechanical axis of the carpus/metacarpus and the joint orientation line of the distal radius/ulna. (5) Mechanical thoracic humeral angle (mTHA): The angle defined by the intersection of the mechanical axis of the humerus and the thoracic limb mechanical axis. (6) Mechanical humeral radioulnar angle (mHRUA): The angle defined by the intersection of the mechanical axis of the humerus and mechanical axis of the radius/ulna. (7) Mechanical radio-ulnar metacarpal angle: The angle defined by the intersection of the mechanical axis of the radius/ulna and the mechanical axis of the carpus/metacarpus. (8) Mechanical thoracic metacarpal angle (mTMCA): The angle defined by the intersection of the thoracic limb mechanical axis and the mechanical axis of the carpus/metacarpus. (9) Elbow mechanical axis deviation (eMAD): The displacement of the elbow relative to the thoracic limb axis, expressed as a percentage of thoracic limb length to normalize for variations in limb size. The distance between the thoracic limb axis and the midpoint of the distal humeral joint reference line was determined by placing a perpendicular line from the mechanical thoracic limb axis to the midpoint of the distal humeral joint orientation line. To normalize for variations in limb length, eMAD was then expressed as a percentage of thoracic limb length (length of the thoracic limb mechanical axis). (10) Carpal mechanical axis deviation (cMAD): The displacement of the carpus from the thoracic limb axis, expressed as a percentage of thoracic limb length to normalize for variations in limb size. The distance between the thoracic limb axis and the midpoint of the distal radius/ulna joint reference line was determined by placing a perpendicular line from the mechanical thoracic limb axis to the midpoint of the distal radius/ulna joint orientation line. As with eMAD, cMAD values were reported as a percentage of limb length. (11) Elbow compression angle (ECA): The angle defined by the intersection of the distal humerus joint reference line and the proximal radius/ulna joint reference line. (12) Elbow rotational position (ERP): ERP (reported as a percentage) was determined by dividing the distance between the medial epicondyle of the humerus and the medial cortex of the olecranon by the distance between the medial and lateral epicondyles of the same elbow.

For the joint orientation angles (mLDHA, mMPRUA, mLDRUA, mLPCMCA), all values were considered positive regardless of whether the angle opened medial or lateral to the center of the joint orientation line. However, for the limb alignment values generated from intersection of mechanical axes of the long bones, SHO often caused these angles to open either medial or lateral to the center of the joint orientation line (i.e., a change in the "polarity" of the angle from opening medial or lateral to the center of the joint orientation line). For this reason, a positive value (+) denoted an angle that opened medial to the center of the joint reference line, whereas a negative value (−) denoted an angle that opened lateral to the center of the joint reference line (Fig 2). A similar convention was used for eMAD and cMAD.

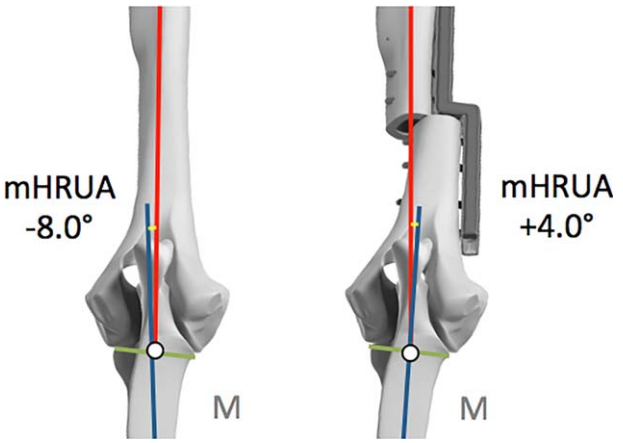

Figure 2 Schematic of the convention by which limb alignment values were assigned positive (+) or negative (−) values. Pre-sliding humeral osteotomy (SHO), the mHRUA opens lateral to the center of the elbow joint orientation line. By convention, angles opening lateral to the center of a joint orientation line are negative (−) values. Post-SHO, mHRUA opens medial to the center of the joint orientation line. By convention, angles opening medial to the center of a joint orientation lien are positive (+) values. This convention is necessary due to the transition of certain limb alignment values across the value 0 (complete coaxial alignment) resulting in the numeric value changing polarity (negative to positive reversal after SHO in the case of mHRUA). M denotes medial. Published with permission of Mr. Tim Vojt.

Statistical Analyses

Descriptive limb alignment statistics were generated for all limbs and reported as mean ± SD and 95% CI by the following groups: pre-SHO vs. post-SHO limb alignment value and limb position (standing vs. recumbent). If present, non-normally distributed data were reported as median and interquartile range. The association between the independent variable (limb) and the dependent variable (difference in limb alignment values pre- and post-SHO) was determined for standing and recumbent positions individually, using a hierarchical mixed effect linear model using a Step-Up Model Building Strategy.[28] The first step was to fit the random effects of "dog" and "the repeated measure of limb within dog" in a model without inclusion of any independent fixed effects. Additionally, homogeneity of variances across limbs (left vs. right) was tested. Likelihood ratio tests (LR) were then used to determine if the random effect and repeated measure improved the fit of each model. If the variance across limbs was not

homogenous, the variance was allowed to vary by left vs. right limbs. The independent variable of limb was next assessed using Type III F-tests. Model diagnostics included visual assessment of the normality assumption of residuals using Q–Q plots as previously described.[28] For limb alignment values where residuals of the final model were not normally distributed (mTMCA), Wilcoxon signed-ranks tests were used to determine the association between limb alignment value and independent variables. To adjust for multiple joint-angle comparisons across 12 limb alignment values, an a priori adjustment to the significance level ($\alpha=0.05$) was calculated using the following formula $\alpha_{adjusted}=\alpha/n$, where n was the number of limb alignment values measured. Thus, $P\leq.004$ was considered significant. Descriptive and analytical statistical analyses were performed using commercial software (Stata/MP 14.1, StataCorp; SAS 9.3, SAS Institute, Cary, NC).

RESULTS

Pilot Study—Effect of Manus Position on Post-SHO Limb Alignment Values

There were no differences in any of the 12 limb alignment values when the 2 loading protocols were directly compared (Supporting Information Table S1). Thus, we elected to proceed with the full study using the second of the 2 post-SHO manus positions (manus allowed to lateralize in response to SHO) as this position is consistent with the clinical observations of some surgeons.

Full Study

The random effect of dog did not improve the fit of any of the limb alignment value models, hence dog as a random effect was not included in the final models. The assumption of homogenous variance for limb (left and right limb) measures was not met for mLPCMCA ($P<.001$) and mRUMCA ($P=.033$) in standing limb position and mHRUA ($P=.027$) and eMAD ($P=.006$) for recumbent limb position. Thus, for these joint-angle measures, the models were adjusted for heterogeneous variance. For the foot lateralization measurement in standing limb position, dog was significant as a random effect ($P<.001$) and the variance for limbs was homogenous.

For the standing limb position, limb alignment values were significantly different pre- and post-SHO for mLDHA, mHRUA, mTHA, eMAD, cMAD, and ECA (Tables 1–3; Figs 3 and 4; $P<.001$ for all). Specifically, SHO resulted in a decrease in the mLDHA, and a movement of the mHRUA, mRUMCA, mTHA, and eMAD toward coaxial alignment of the limb. In contrast, cMAD moved away from coaxial alignment of the limb post-SHO. The manus underwent significant lateralization from 3.0 ± 0.7 cm pre-SHO to 4.4 ± 1.1 cm post-SHO (Figs 5 and 6; $P<.001$). For the recumbent limb position, limb alignment values for mLDHA, mHRUA, mRUMCA, mTHA, eMAD, and ERP were significantly different ($P<.001$ for all) pre- and post-SHO (Tables 1–3), following the general pattern described above for the standing limb position.

DISCUSSION

Using an ex vivo limb press model to evaluate frontal plane thoracic limb alignment pre- and post-SHO in simulated standing and recumbent positions, we were unable to support the null hypothesis that SHO would have no effect on thoracic limb alignment. Indeed, in both standing and recumbent limb positions, 6 of the 12 frontal plane thoracic limb alignment values moved toward the value '0' (representing coaxial alignment) after SHO. These results suggest that SHO not only affects the position of the humerus and elbow

Table 1 Pre- and post-sliding humeral osteotomy joint orientation angles (°) for standing and recumbent limb positions

	Standing				
	Mean ± SD			95% CI	
Limb alignment value	Pre	Post	*P*-value	Pre	Post
Mechanical lateral distal humeral angle (mLDHA)	87.6 ± 3.2	83.5 ± 2.7	<.001	86.4–88.8	82.5–84.5
Mechanical medial proximal radio-ulnar angle (mMPRUA)	81.0 ± 2.8	81.5 ± 3.2	.033	79.9–82.0	80.3–82.7
Mechanical lateral distal radio-ulnar angle (mLDRUA)	87.0 ± 2.7	87.8 ± 1.9	.065	86.0–88.0	87.1–88.5
Mechanical lateral proximal carpal-metacarpal angle (mLPCMCA)	80.6 ± 5.8	78.8 ± 5.7	.845	78.5–82.8	76.7–81.0
	Recumbent				
	Mean ± SD			95% CI	
Limb alignment value	Pre	Post	*P*-value	Pre	Post
Mechanical lateral distal humeral angle (mLDHA)	86.8 ± 2.3	82.8 ± 2.1	<.001	85.9–87.7	82.0–83.6
Mechanical medial proximal radio-ulnar angle (mMPRUA)	81.8 ± 2.9	81.2 ± 3.0	.162	80.7–82.9	80.1–82.4
Mechanical lateral distal radio-ulnar angle (mLDRUA)	87.1 ± 3.7	88.2 ± 3.1	.091	85.8–88.5	87.0–89.4
Mechanical lateral proximal carpal-metacarpal angle (mLPCMCA)	86.5 ± 4.5	87.5 ± 4.0	.089	84.8–88.2	86.0–89.0

Table 2 Pre- and post-sliding humeral osteotomy limb alignment values for standing and recumbent limb positions

	Standing				
	Mean ± SD			Mean ± SD	
Limb alignment value	Pre	Post	*P*-value	Pre	Pre
Mechanical humeral radio-ulnar angle (mHRUA)	(−)10.7 ± 3.8	(−)5.4 ± 4.4	<.001	(−)12.1–(−)9.3	(−)7.0–(−)3.8
Mechanical radio-ulnar metacarpal angle (mRUMCA)*	12.4 ± 3.8	12.9 ± 5.5	.048	11.0–13.8	10.9–15.0
Mechanical thoracic humeral angle (mTHA)	4.0 ± 2.8	0.9 ± 2.9	<.001	2.9–5.0	(−)0.2–2.0
Mechanical thoracic metacarpal angle (mTMCA)	(−)5.4 ± 6.1	(−)6.1 ± 9.7	.259	(−)7.7–(−)3.1	(−)9.8–(−)2.5
	Recumbent				
	Mean ± SD			95% CI	
Limb alignment value	Pre	Post	*P*-value	Pre	Post
Mechanical humeral radio-ulnar angle (mHRUA)	(−)8.9 ± 3.9	(−)4.8 ± 3.6	<.001	(−)10.4–(−)7.4	(−)6.2–(−)3.5
Mechanical radio-ulnar metacarpal angle (mRUMCA)	5.9 ± 2.9	4.2 ± 2.6	<.001	4.8–7.0	3.2–5.2
Mechanical thoracic humeral angle (mTHA)	3.6 ± 2.4	1.6 ± 2.0	<.001	2.7–4.5	0.8–2.3
Mechanical thoracic metacarpal angle (mTMCA)	(−)1.6 ± 3.5	(−)0.9 ± 3.7	.524	(−)2.9–(−)0.3	(−)2.3–0.5

Positive values denote an angle that opened medial to the center of the joint reference line. Negative values (−) denote an angle that opened lateral to the center of the joint reference line.
*Limb was significant in model for mRUMCA.

joint, but that in the ex vivo setting, SHO had more widespread effects on alignment of the entire thoracic limb.

The methods used in our study related to the position of the manus in relationship to the humeral head pre- and post-SHO warrant explanation. In the pre-SHO standing limb position, the manus was allowed to freely contact the baseplate and a plumb line was used to confirm that the center of the manus was located beneath the center of the humeral head. These 2 structures represent the distal and proximal most aspect of the thoracic limb mechanical axis, respectively. Positioning of the limb in this manner allowed axial loads to be applied to the entire limb. However, SHO resulted in slight, albeit significant, lateralization of the manus due to the disparity in the distance between the medial cortex of the humerus at the osteotomy vs. the distal most aspect of the plate. One potential method to address this alteration would have been to re-align the manus directly beneath the humeral head after SHO, such that the manus

Table 3 Mechanical axis deviation (%), elbow compression angle (°), elbow rotational position (%), and foot lateralization (cm) values for standing and recumbent limb positions

	Standing				
	Mean ± SD			95% CI	
Limb alignment value	Pre	Post	*P*-value	Pre	Post
Elbow mechanical axis deviation (eMAD)	2.8 ± 1.6	0.7 ± 1.8	<.001	2.2–3.4	0.03–1.4
Carpus mechanical axis deviation (cMAD)	(−)1.8 ± 1.0	(−)2.3 ± 1.3	<.001	(−)2.2–(−)1.4	(−)2.8–(−)1.8
Elbow compression angle (ECA)	2.7 ± 1.6	1.4 ± 1.5	<.001	2.1–3.3	0.9–2.0
Elbow rotational position (ERP)	0.4 ± 0.03	0.4 ± 0.02	.849	0.4–0.5	0.4–0.4
Foot lateralization	3.0 ± 0.7	4.4 ± 1.1	<.001	2.8–3.3	4.0–4.9
	Recumbent				
	Mean ± SD			95% CI	
Limb alignment value	Pre	Post	*P*-value	Pre	Post
Elbow mechanical axis deviation (eMAD)	2.6 ± 1.6	1.0 ± 1.4	<.001	2.0–3.2	0.4–1.5
Carpus mechanical axis deviation (cMAD)	(−)0.4 ± 1.0	(−)0.7 ± 0.8	.059	(−)0.8–(−)0.02	(−)1.0–(−)0.4
Elbow compression angle (ECA)	1.7 ± 1.4	1.1 ± 1.5	.058	1.1–2.2	0.6–1.7
Elbow rotational position (ERP)	0.4 ± 0.03	0.5 ± 0.03	<.001	0.4–0.4	0.4–0.5
Foot lateralization	N/A	N/A	N/A	N/A	N/A

Positive values denote an angle that opened medial to the center of the joint reference line. Negative values (−) denote an angle that opened lateral to the center of the joint reference line. Foot lateralization was determined by physical measurement of the position of the manus pre- and post-SHO in standing limb position only, rather than using radiographic measurements.

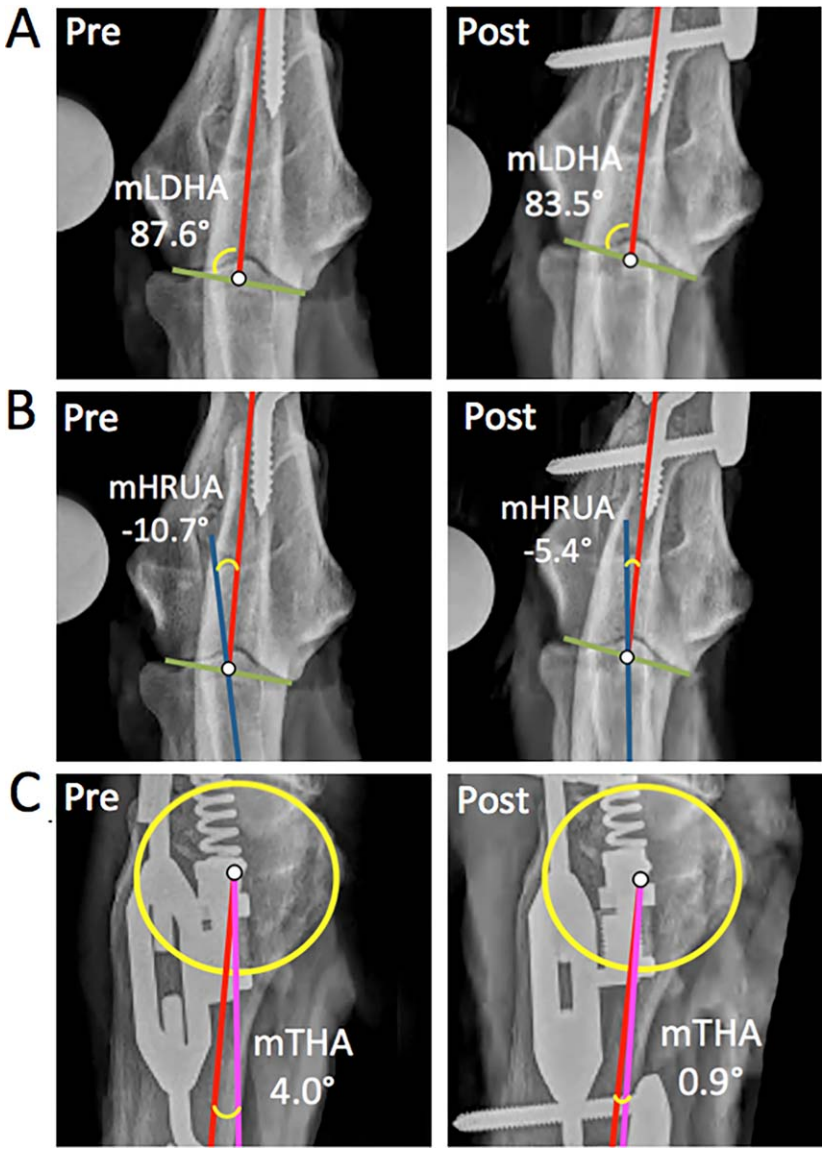

Figure 3 Representative radiographs of limb alignment measurements pre- and post-sliding humeral osteotomy (SHO). (A) mLDHA: mechanical lateral distal humeral angle, or the angle formed by the mechanical axis of the humerus (red) and joint orientation line of the distal humerus (green). (B) mHRUA: mechanical humeral radio-ulnar angle, or the angle formed by the intersection of the mechanical axes of the humerus (red) and radius/ulna (blue). By convention, mHRUA is negative due to the fact that the angle opens lateral to the center of the joint reference line. (C) mTHA: mechanical thoracic humeral angle, or the angle formed by the intersection of the mechanical axes of the humerus (red) and the thoracic limb (magenta).

and humeral head were axially aligned once again, allowing pure axial loading of the limb. However, manipulation of the manus and limb in this manner may not represent the clinical scenario in dogs post-SHO. Unfortunately, the location and placement of the manus after SHO in vivo has yet to be determined. However, some SHO surgeons have observed that many dogs will initially walk with the limb and manus slightly lateralized after SHO and that this change diminishes with time (personal communications, Dr. Brian Beale, Gulf Coast Veterinary Specialists, Houston, TX). This concept is consistent with findings related to foot position in people after high tibial osteotomy, namely that some patients place the foot of the operated limb in an altered position after surgery.[29–31] We thoughtfully considered these findings and prior to initiation of the present study and performed the pilot study described above to assess the effect of manus position on limb alignment values post-SHO. Although it could be argued that the differences in limb alignment values we report after SHO in the standing limb position are attributable to our loading protocol, we demonstrated that manus position during limb loading does not appear to have an effect on any of the 12 limb alignment values in our pilot

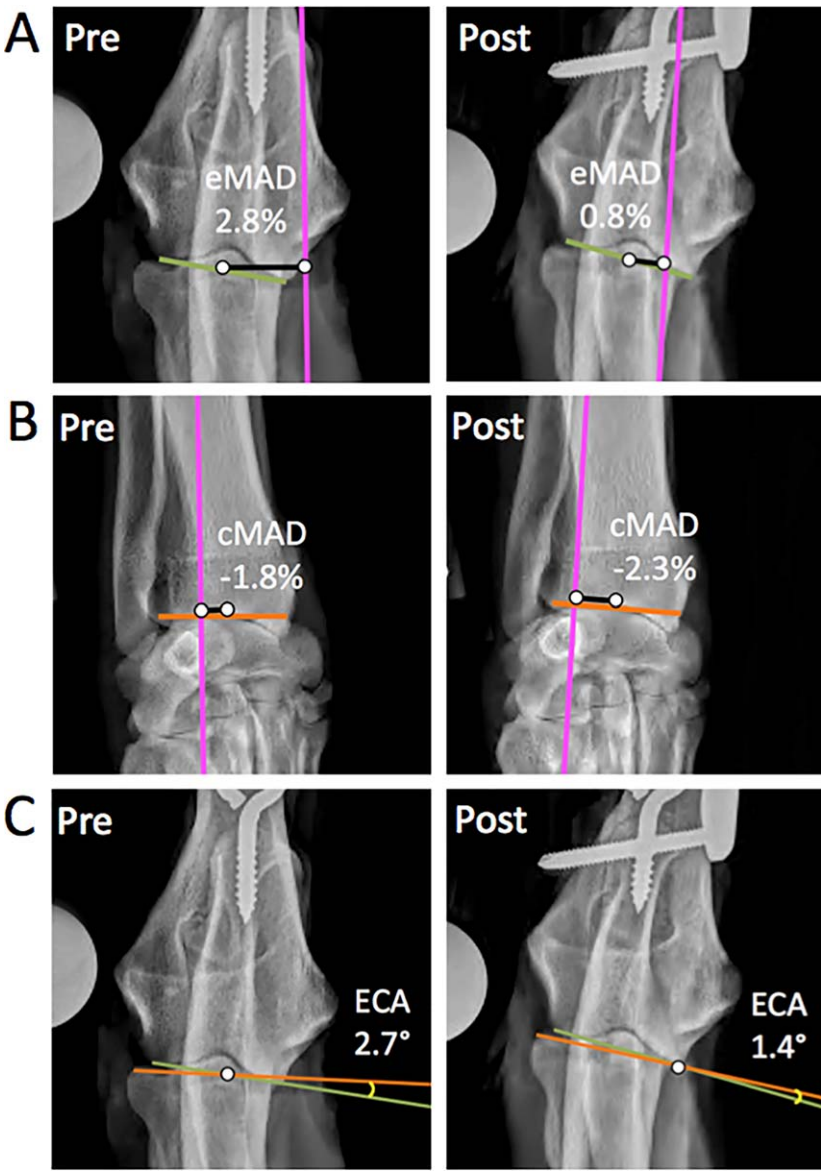

Figure 4 Representative radiographs of limb alignment measurements pre- and post-sliding humeral osteotomy (SHO). (A) eMAD: elbow mechanical axis deviation, or the relative displacement (black line) of the center of the elbow (determined by the center of the green joint reference line) from the mechanical axis of the thoracic limb (magenta). To control for differences in dog and limb size, eMAD is normalized to individual limb length and reported as a percentage deviation relative to overall limb length. (B) cMAD: carpus mechanical axis deviation, or the relative displacement (black line) of the center of the carpus (determined by the center of the orange joint reference line) from the mechanical axis of the thoracic limb (magenta). As with eMAD, cMAD is reported as a percentage deviation relative to overall limb length. By convention, cMAD is negative due to the fact that the center of the carpus displaces medial to the mechanical axis of the limb. (C) ECA: elbow compression angle, or the angle of intersection, if present, between the distal humeral joint reference line (green) and proximal radius/ulna joint reference line (orange).

study. Furthermore, there were significant differences in 6 of the 12 frontal plane thoracic limb alignment values post-SHO when assessed using recumbent caudocranial radiographic montages, confirming that the alterations in limb alignment we report are not solely due to our standing limb methodology.

We previously demonstrated that limb alignment values are significantly different when determined from standing vs. recumbent radiographs in a population of healthy Labrador Retrievers.[24] While standing radiography may prove to be of particular use in the clinical setting in regards to diagnosis, decision-making, and outcome assessment of limb alignment procedures used to treat MCD, we currently lack data to support this concept. For this reason, we evaluated the effect of SHO on limb alignment in both recumbent and standing limb positions to mirror our prior in vivo work. We also included recumbent radiography due to the fact that standing radiography requires horizontal beam capabilities

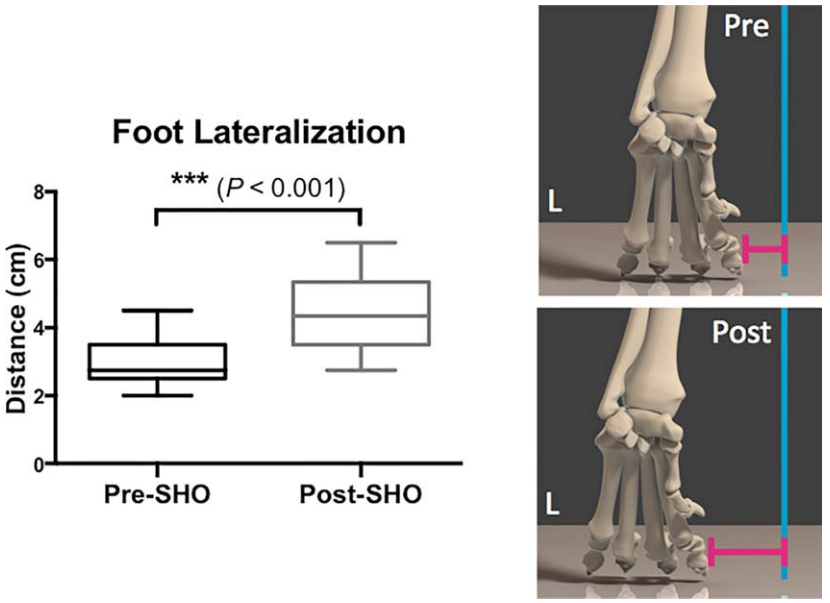

Figure 5 Box and whisker plot and schematic of foot position pre- and post-sliding humeral osteotomy (SHO). The box denotes lower and upper quartiles, the horizontal bar the median, and the vertical bars range. Position of the manus was determined for each limb using a 1 cm × 1 cm textured grid in a simulated standing position pre-SHO (Pre) relative to a plumb line dropped from the medial aspect of the upper test fixture (turquoise line). After SHO, the position of the manus was again determined (Post). There was a significant increase in foot lateralization after SHO. L denotes lateral. Published with permission of Mr. Tim Vojt.

not universally present in all veterinary practices. As such, recumbent radiographs may prove to be more widely available in a clinical setting and warrant continued evaluation in future clinical studies.

The impact of this study is twofold. First, using an ex vivo study design, we demonstrated that SHO affected thoracic limb alignment values involving the elbow, mechanical axis of the humerus, radius/ulna, and the mechanical axis of the thoracic limb. Second, the standing and recumbent frontal plane thoracic limb alignment methodology used to document these limb alignment changes is likely to be useful for preoperative screening, surgical decision making, and postoperative outcome assessment in client owned dogs treated with SHO or other osteotomies purported to reduce loading of the medial aspect of the elbow.

We speculate that the significant reduction in mLDHA occurred due to the lateral tilt of the distal humeral fragment during tightening of the SHO plate cortex screws, which occurred due to the disparity in the distance between the medial cortex of the humerus and the undersurface of the SHO plate. During SHO screw tightening, translation of the mechanical axis of the distal humerus first occurs in a lateral to medial direction, resulting in a humeral long axis shift similar to the tibial long axis shift described by Kowaleski et al.[32] However, a subsequent rotation or tilting of the epiphysis of the humerus in a lateral direction occurs next, once the distal humerus contacts the distal aspect of the SHO plate. We suggest that both of these events are responsible for the reduction in mLDHA.

Both mHRUA and mTHA were significantly different when determined using standing and recumbent radiographs. The movement of mHRUA and mTHA toward a value of '0' after SHO represents a movement toward co-axial alignment of the mechanical axes of the humerus, radius/ulna and the mechanical axis of the thoracic limb. We believe the alterations in these values likely occur secondary to reduction in mLDHA. SHO also induced significant changes in both ECA and foot position. ECA decreased significantly after SHO, but only in the simulated standing limb position. This suggests that the joint surfaces of the humerus and radius/ulna moved toward a more parallel position after SHO, which is consistent with prior ex vivo work reporting translation of joint forces from the medial to the lateral joint surface.[8,13]

In our original study, we detailed the technique to determine 12 frontal plane thoracic limb alignment values using standing and recumbent radiography.[24] Interestingly, while 6 of these same limb alignment values were affected by SHO, other values did not significantly change in response to SHO. The authors speculate that values such as mMPRUA, mLDRUA, mLPCMCA, mRUMCA (standing position only), and mTMCA did not change significantly due the fact that these limb alignment values are associated with the mechanical axes of the radius/ulna, metacarpus, and the lower thoracic limb. Indeed, the fact that our systematic technique of determining thoracic limb alignment detected significant differences primarily in limb alignment values involving the humerus, elbow, and intersection of the

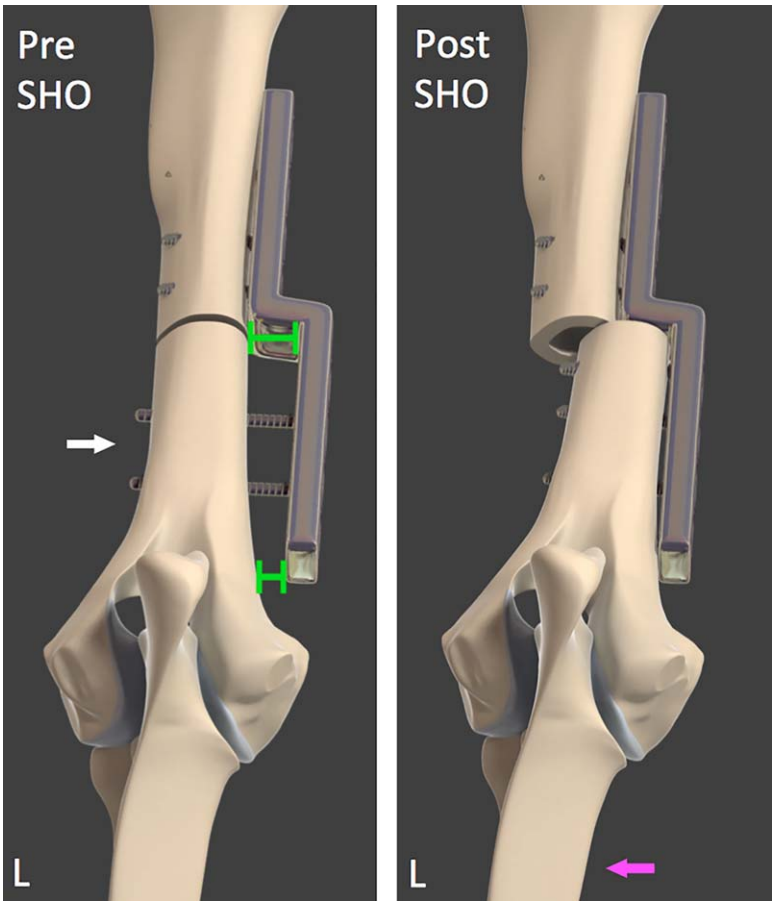

Figure 6 Illustration of the relationship between the medial surface of the humerus and the undersurface of the sliding humeral osteotomy (SHO) plate pre- and post-SHO. Due to alterations in normal humeral anatomy, the diameter of the humerus mid-diaphysis is smaller than the diameter of the humerus distally beneath the distal most aspect of the SHO plate. This causes a disparity in the distance between the medial cortex of the humerus and the undersurface of the SHO plate, as denoted by the green bars. The white arrow indicates the direction of translation of the distal humerus during SHO. As the distal cortex screws are tightened, the distal humerus translates medially. Upon contact of the distal humerus with the distal most aspect of the plate, translation of the distal humerus ceases, while the humerus adjacent to the osteotomy continues to translate until both the proximal and distal aspects of the distal humerus are in contact with the SHO plate. This leads to additional rotation or tilting of the distal humerus and rotation of the distal humerus from a medial to lateral direction in the sagittal plane (magenta arrow). L denotes lateral. Published with permission of Mr. Tim Vojt.

mechanical axes of the humerus and radius and ulna demonstrates the fidelity of our methodology.

In people, the mechanical axis of the lower extremity lies slightly medial to the center of the knee.[18] The relationship between the center of the knee and the mechanical axis of the limb is defined by the mechanical axis deviation, or MAD. In people with medial knee gonarthrosis, alterations in MAD are associated with collapse of the medial compartment of the knee and concurrent proximal tibial varus. A goal of high tibial osteotomies is to move the mechanical axis of the limb toward the center of the knee, thereby reducing MAD and transferring loads toward a less severely affected lateral joint compartment.[10,19] In our study, we report a significant decrease in eMAD after SHO, demonstrating that the mechanical axis of the canine thoracic limb moves in a medial to lateral direction in a similar manner. Thus, eMAD (as well as mLDHA, mHRUA, mTHA, and ECA) may prove useful in the clinical setting for the development of more objective case selection guidelines for SHO or in evaluation of efficacy after surgery.

Admittedly, it is currently unknown whether use of thoracic limb alignment for surgical decision-making or outcome assessment in clinically affected dogs will prove to be useful. While one can speculate that the SHO may result in permanent decrease in the loading of the medial compartment of the elbow in vivo, the effect of SHO could also be short-lived. The position of the manus after surgery has been noted to move from a lateralized to a more centralized position at long-term follow-up in some dogs (personal communications, Dr. Brian Beale). Cleary, much additional work is needed to pursue these questions and will be the focus of future clinical studies.

As with all studies, ours was not without limitations. We used an ex vivo cadaveric model based on adaptations from prior work.[26,33,34] Lack of muscle tone and

proprioceptive response during limb positioning as well as ligament/tendon laxity prevent us from translating our results directly to the clinical setting. Albeit unlikely, it is possible that the changes in standing thoracic limb alignment we describe occurred due to the removal and re-mounting of specimens in the limb press pre- and post-SHO. We ensured that the position of the proximal humerus pre- and post-SHO was identical by the use of index marks adjacent to the upper test fixture. Furthermore, we documented significant changes when limb alignment was assessed using recumbent radiographic positions. Several recent studies have reported changes in elbow contact area and pressure in response to osteotomies of the humerus or ulna.[8,13,26,34,35] The objective of our study was to determine if thoracic limb alignment changed in response to SHO, not to evaluate contact pressure or area in response to SHO. Evaluation of contact mechanics in our model using pressure sensor systems would have required additional dissection of medial and lateral tissues adjacent to the joint. Furthermore, it has been reported that the use of pressure sensors is fraught with challenges and potential data recording errors when used in a small, confined, curvilinear joint spaces.[36,37] Given the fact that our long-term goal is to develop a noninvasive, widely available system to evaluate osteotomy procedures in clinical cases, we elected to focus our efforts on radiography and thoracic limb alignment in this initial ex vivo proof of concept study.

In conclusion, in the ex vivo setting, SHO was associated with significant alterations in thoracic limb alignment when assessed using both standing and recumbent limb positions. The results of our study suggest a novel mechanism by which SHO might assert clinical effects in vivo, namely through alteration of thoracic limb alignment as has been documented in high tibial osteotomies in people.[9,10,38,39] Future work is necessary to determine whether the differences in limb alignment described in our ex vivo study occur after SHO in the clinical setting.

ACKNOWLEDGMENT

The authors wish to acknowledge Mr. Jeff Harris at the Southwest Research Institute for his expertise in fabrication of the limb press and Dr. Kayla Corriveau for assistance with the experimental stage of the study. This work was funded by the Veterinary Orthopedic Society's Wade O. Brinker Resident Research Award (2015) and the Ginn Fund, Texas A&M University. Partial funding for the canine limb press was kindly provided by Franco Dibartolo (InTrauma, Rivoli, Italy). Surgical implants were provided by New Generation Devices (Glen Rock, NJ).

DISCLOSURE

The authors declare no conflicts of interest related to this report.

REFERENCES

1. Boulay JP: Fragmented medial coronoid process of the ulna in the dog. *Vet Clin North Am Small Anim Pract* 1998;28:51–74
2. Meyer-Lindenberg A, Langhann A, Fehr M, et al: Prevalence of fragmented medial coronoid process of the ulna in lame adult dogs. *Vet Rec* 2002;151:230–234
3. Vermote KAG, Bergenhuyzen ALR, Gielen I, et al: Elbow lameness in dogs of six years and older. Arthroscopic and imaging findings of medial coronoid disease in 51 dogs. *Vet Comp Orthop Traumatol* 2010;23:43–50
4. Fitzpatrick N, Yeadon R: Working algorithm for treatment decision making for developmental disease of the medial compartment of the elbow in dogs. *Vet Surg* 2009;38:285–300
5. Schulz KS: Diagnostic assessment of the elbow. When in doubt, scope the elbow. *Proc American College of Veterinary Surgeons Symposium*, Denver, CO, 2004, pp 239–231
6. Kramer A, Holsworth I, Wisner E, et al: Computed tomographic evaluation of canine radioulnar incongruence in vivo. *Vet Surg* 2006;35:24–29
7. Wind AP: Elbow incongruity and developmental elbow disease in the dog. *J Am Anim Hosp Assoc* 1986;22:725–730
8. Fujita Y, Schulz KS, Mason DR, et al: Effect of humeral osteotomy on joint surface contact in canine elbow joints. *Am J Vet Res* 2003;64:506–511
9. Giagounidis EM, Sell S: High tibial osteotomy: factors influencing the duration of satisfactory function. *Arch Orthop Trauma Surg* 1999;119:445–449
10. Amis AA: Biomechanics of high tibial osteotomy. *Knee Surg Sport Tr A* 2012;21:197–205
11. Niemeyer P, Koestler W, Kaehny C, et al: Two-year results of open-wedge high tibial osteotomy with fixation by medial plate fixator for medial compartment arthritis with varus malalignment of the knee. *Arthroscopy* 2008;24:796–804
12. Watanabe K, Tsuchiya H, Sakurakichi K, et al: Acute correction using focal dome osteotomy for deformity about knee joint. *Arch Orthop Trauma Surg* 2008;128:1373–1378
13. Mason D, Schulz K, Fujita Y, et al: Measurement of humeroradial and humeroulnar transarticular joint forces in the canine elbow joint after humeral wedge and humeral slide osteotomies. *Vet Surg* 2008;37:63–70
14. Fitzpatrick N, Yeadon R, Smith T, et al: Techniques of application and initial clinical experience with sliding humeral osteotomy for treatment of medial compartment disease of the canine elbow. *Vet Surg* 2009;38:261–278
15. Fitzpatrick N, Bertran J, Solano MA: Sliding humeral osteotomy: medium-term objective outcome measures and reduction of complications with a modified technique. *Vet Surg* 2014;44:137–149
16. Hernigou P, Medevielle D, Debeyre J, et al: Proximal tibial osteotomy for osteoarthritis with varus deformity. *J Bone Joint Surg Am* 1987;69:332–354
17. Paley D: Realignment for mono-compartment osteoarthritis of the knee, in Herzenberg JE (ed): *Principles of deformity correction*. New York, NY, Springer, 2002, pp 479–503
18. Paley D, Herzenberg JE, Tetsworth K, et al: Deformity planning for frontal and sagittal plane corrective osteotomies. *Orthop Clin North Am* 1994;25:425–465

19. Amer A, Khanfour AA: Evaluation of treatment of late-onset tibia vara using gradual angulation translation high tibial osteotomy. *Acta Orthopaedica Belgica* 2010;76: 360–366
20. Leach RE, Gregg T, Siber FJ: Weight-bearing radiography in osteoarthritis of the knee. *Radiology* 1970;97:265–268
21. Wood MC, Fox DB, Tomlinson J: Determination of the mechanical axis and joint orientation lines in the canine humerus: a radiographic cadaveric study. *Vet Surg* 2014;43: 414–417
22. Fox DB, Tomlinson JL, Cook JL, et al: Principles of uniapical and biapical radial deformity correction using dome osteotomies and the center of rotation of angulation methodology in dogs. *Vet Surg* 2006;35:67–77
23. Tomlinson J, Johnston SA: Normal radial and ulnar joint angles. Proc AO Masters Course on Advanced Osteotomy, Small Animal, La Jolla, CA, 2009, pp 18–21
24. Goodrich ZJ, Norby B, Eichelberger BM, et al: Thoracic limb alignment in healthy Labrador Retrievers: evaluation of standing versus recumbent frontal plane radiography. *Vet Surg* 2014;43:791–803
25. Preston CA, Schulz KS, Kass PH: In vitro determination of contact areas in the normal elbow joint of dogs. *Am J Vet Res* 2000;61:1315–1321
26. Cuddy LC, Lewis DD, Kim SE, et al: Contact mechanics and three-dimensional alignment of normal dog elbows. *Vet Surg* 2012;41:818–828
27. Clements DN, Owen MR: Kinematic analysis of the gait of 10 Labrador Retrievers during treadmill locomotion. *Vet Rec* 2005; 156:478–781
28. West BT, Welch KB, Galecki AT: Three-level models for clustered data-the classroom example, in West BT (ed): *Linear mixed models: a practical guide using statistical software* (ed 2). Boca Raton, FL, Taylor & Francis Group, 2015, pp 135–198
29. Prodromos CC, Andriacchi TP, Galante JO: A relationship between gait and clinical changes following high tibial osteotomy. *J Bone Joint Surg Am* 1985;67: 1188–1194
30. Wang JW, Kuo KN, Andriacchi TP, et al: The influence of walking mechanics and time on the results of proximal tibial osteotomy. *J Bone Joint Surg Am* 1990;72:905–909
31. Goh JCH, Bose K, Khoo BCC: Gait analysis study on patients with varus osteoarthrosis of the knee. *Clin Orthop Relat Res* 1993;294:223–231
32. Kowaleski MP, McCarthy R: Geometric analysis evaluating the effect of tibial plateau leveling osteotomy position on postoperative tibial plateau slope. *Vet Comp Orthop Traumatol* 2004;17:30–34
33. Gutbrod A, Guerrero TG: Effect of external rotational humeral osteotomy on the contact mechanics of the canine elbow joint. *Vet Surg* 2012;41:845–852
34. Cuddy LC, Lewis DD, Kim SE, et al: Ex vivo contact mechanics and three-dimensional alignment of normal dog elbows after proximal ulnar rotational osteotomy. *Vet Surg* 2012;41:905–914
35. Krotscheck U, Kalafut S, Meloni G, et al: Effect of ulnar ostectomy on intra-articular pressure mapping and contact mechanics of the congruent and incongruent canine elbow ex vivo. *Vet Surg* 2014;43:339–346
36. Drewniak EI, Crisco JJ, Spenciner DB, et al: Accuracy of circular contact area measurements with thin-film pressure sensors. *J Biomech* 2007;40:2569–2572
37. Wilharm A, Hurschler C, Dermitas T, et al: Use of tekscan k-scan sensors for retropatellar pressure measurement avoiding errors during implantation and the effects of shear forces on the measurement precision. *Biomed Res Int* 2013; 2013:1–7
38. Waterman BR, Hoffmann JD, Laughlin MD, et al: Success of high tibial osteotomy in the United States military. *Orthop J Sports Med* 2015;3:1–6
39. Howells NR, Salmon L, Waller A, et al: The outcome at ten years of lateral closing-wedge high tibial osteotomy. *Bone Joint J* 2014;96-B:1491–1497

SUPPORTING INFORMATION

Additional Supporting Information may be found in the online version of this article at the publisher's website:

Table S1 Results of a pilot study (n=5 limbs) assessing the potential effect of manus position on limb alignment values (°) and mechanical axis deviations (%) post-sliding humeral osteotomy (SHO).